Journal of Information Systems Engineering and Management
2025, 10(25s)
e-ISSN: 2468-4376
https://www.jisem-journal.com/

Research Article

Sensorless Speed Estimation of Induction Motor using ANFIS

Dicky Rivaldo Ramdani [1], Novie Ayub Windarko [1], Era Purwanto[1]
[1]*Electrical Engineering Department, Politeknik Elektronika Negeri Surabaya, Sukolilo, Surabaya, Indonesia*
E-mail: ramdanidicky78@gmail.com, ayub@pens.ac.id, era@pens.ac.id

ARTICLE INFO

Received: 26 Dec 2024

Revised: 12 Feb 2025

Accepted: 22 Feb 2025

ABSTRACT

In modern industrial applications, particularly in the era of Industry 5.0, accurate estimation of induction motor speed is essential for ensuring optimal performance, energy efficiency, and system reliability. Traditional methods using mechanical sensors for speed measurement are often limited by increased system complexity, high maintenance costs, and vulnerability to environmental conditions. This study presents a sensor less approach for predicting the acceleration for the induction motor with ANFIS, an Adaptive Neuro-Fuzzy Inference Technology. ANFIS integrates the learning capabilities of neural networks with the inferential benefits of fuzzy logic, making it suitable for nonlinear systems and uncertain environments. The study entails the creation and training of an ANFIS model utilizing motor data. The model employs many membership functions, such as Trimf, Trapmf, Gbellmf, and Gaussmf, and the assessment utilized RMSE to evaluate their efficacy. The findings reveal that the Trimf membership function yields the highest predictive accuracy, with an RMSE of 0.0187, whilst the Trapmf function shows the lowest accuracy, with an RMSE of 0.0213. The ANFIS system successfully estimates motor speed with minimal deviation from the actual output, as observed in simulations. This sensor less approach not only reduces costs and complexity but also supports the development of intelligent, energy-efficient systems in line with Industry 5.0 objectives. Overall, the findings highlight the potential of ANFIS for advanced motor control applications, contributing to smarter automation and improved sustainability.

Keywords: ANFIS, Induction Motor, Sensorless Estimation, Membership Function, Industry 5.0.

I. INTRODUCTION

Induction motors remain a cornerstone in industrial applications, prized for their robustness, cost-effectiveness, and low maintenance requirements [1]. In the era of Industry 5.0, accurate speed estimation of induction motors has become increasingly crucial for enhancing control precision, optimizing energy efficiency, and enabling predictive maintenance strategies [2], [3].

The implementation of physical speed sensors, although yielding precise data, frequently incurs extra expenses, diminishes system reliability, and complicates motor design [4], [5]. This has resulted in an increasing interest in sensorless control methodologies, wherein speed is inferred rather than directly measured. Among these approaches, those employing widely accessible electrical parameters such as stator currents (Id, Iq) and voltages (Vd, Vq) in the d-q reference frame have garnered considerable attention due to their non-invasive characteristics and potential for high precision [6].

Conventional speed estimate techniques, such as MRAS (model reference adaptive systems) and EKF (extended Kalman filters), have been thoroughly investigated [7], [8]. However, these approaches often face challenges when dealing with parameter variations and system nonlinearities, leading to reduced accuracy under certain operating conditions. Recent breakthroughs in artificial intelligence and machine learning have created fresh opportunities to overcome these restrictions. [9].

The Adaptive Neuro-Fuzzy Inference System (ANFIS) has become a formidable instrument in intelligent control and estimate. [4]. ANFIS integrates the learning capabilities of neural networks with the reasoning power of fuzzy logic, providing a robust framework for managing complicated, nonlinear systems like induction motors [5]. The ability of

ANFIS to effectively map the relationship between electrical parameters (Idq, Vdq) and motor speed makes it particularly suitable as a speed sensor replacement [6], [7].

Recent studies have demonstrated the potential of ANFIS in various aspects of electrical machine control and estimation [8], [9]. The use of ANFIS for speed estimation using Idq and Vdq as inputs offers several advantages:

1. It eliminates the need for additional hardware sensors, reducing system cost and complexity [10].
2. It can adapt to motor parameter variations and nonlinearities more effectively than conventional methods [11].
3. It provides a robust estimation even under varying load conditions and speeds [12].
4. It can be easily integrated into existing motor drive systems without significant hardware modifications [13].

Despite these advancements, designing an effective ANFIS-based speed estimator for induction motors still presents several challenges. These include selecting optimal input variables, fine-tuning the network structure, and ensuring estimator robustness across diverse operating conditions [14]. The amalgamation of ANFIS with nascent technologies like edge computing and the Internet of Things (IoT) introduces novel potential and difficulties within the realm of smart manufacturing [15].

This research aims to address these challenges by developing an innovative ANFIS-based speed estimation system for induction motors, specifically utilizing Idq and Vdq as input parameters. The proposed design focuses on:

1. Optimizing the ANFIS structure to effectively map the relationship between Idq, Vdq, and motor speed.
2. Developing a robust training algorithm that ensures accurate speed estimation across a wide range of operating conditions.
3. Implementing real-time adaptation mechanisms to handle motor parameter variations and external disturbances.

By achieving these objectives, this study seeks to contribute to the advancement of sensorless techniques for induction motors, potentially leading to improved efficiency, reliability, and adaptability in modern industrial applications

II. MATERIALS AND METHOD

This research focuses on the use of 3-phase induction motors as the main object of study. The motor chosen for this study is the squirrel-cage type, which is known for its simple construction and reliability. Tests were conducted on this motor to observe and analyze the speed changes that occur. This research consists of two main interrelated stages:

A. System Design and Manufacturing Stage

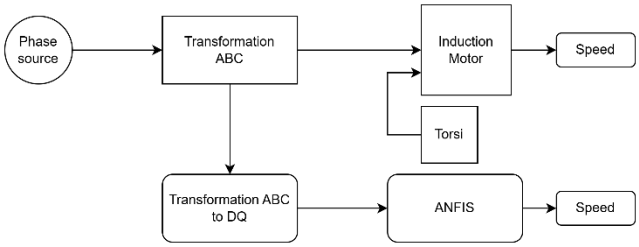

Figure 1 system block diagram

The diagram represents a control system utilizing ANFIS to manage the speed of an induction motor. Key components of the system include a three-phase voltage source as the input, a transformation block that converts ABC coordinates into the DQ domain for signal processing, and an induction motor as the primary actuator. The motor provides torque and speed as output, which are used as feedback for the control loop. The ANFIS module is responsible for adjusting the motor speed according to a specified reference. This setup allows for precise and adaptive speed control of the induction motor.

A three-phase induction motor's dynamic behaviour can be characterized by differential equations derived from the motor's equivalent circuit [8]. These equations are often expressed in terms of direct and components along the quadrature axis (d-q components) within a reference frame that remains stable [9]. The d-q model simplifies the analysis by transforming the three-phase quantities into two orthogonal components [10].

The voltage equations for the stator and rotor circuits in the d-q frame are given by:

$$\mathbf{V_{qs}^s = R_s I_{qs}^s + \frac{d}{dt}\varphi_{qs}^s} \quad (1)$$

$$\mathbf{V_{ds}^s = R_s I_{ds}^s + \frac{d}{dt}\varphi_{ds}^s} \quad (2)$$

Where:

- V_{ds},V_{qs} are the direct and quadrature axis stator voltage
- R_s are the stator and rotor resistance

The flux linkages are related to the currents by:

$$\mathbf{\varphi_{qs}^s = L_{ls} I_{qs}^s + L_m I_{qm}} \quad (3)$$

$$\mathbf{\varphi_{ds}^s = L_{ls} I_{ds}^s + L_m I_{dm}} \quad (4)$$

$$\mathbf{\varphi_{qr}^s = L_{lr} I_{qr}^s + L_m I_{qm}} \quad (5)$$

$$\mathbf{\varphi_{dr}^s = L_{lr} I_{dr}^s + L_m I_{dm}} \quad (6)$$

The electromagnetic torque T_e produced by the motor is given by:

$$T_e = \frac{3}{2}\frac{P}{2}\frac{L_m}{L_r}\left(\varphi_{dr}^s\left(I_{qs}^s - I_{qa}\right) - \varphi_{qr}^s\left(I_{ds}^s - I_{da}\right)\right) \quad (7)$$

where P is the number of poles

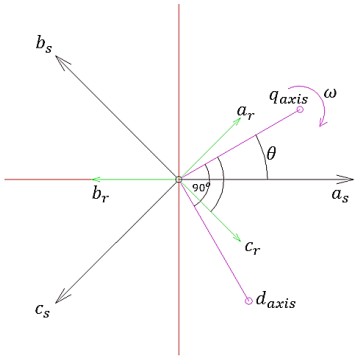

Figure 2 Relationship between ABC Transformation and dq0 in Stationary Reference Frame [16]

It is presumed that a 3-phase induction motor is symmetrical. The reference frame dq0 is typically positioned based on the location of the motor analysis components employed. This study employs a dynamic model of an induction motor with a stationary reference frame designated as dq0 [16]. To transform the abc condition into dq0, the first thing to do is to determine the direction of rotation of the rotor in the stationary condition (unchanged) [10]. In this condition, the relation between the abc magnitude and the dq0 magnitude at the stationary reference when the speed is equal can be seen in Figure 2 The notation shows the abc phase magnitude on the rotor, the notation shows the abc phase magnitude on the stator, and the dq axis shows the dq0 transformation magnitude[9].

The magnitude of the transformation of abc to dq0 with a stationary frame of reference is shown in equation (8):

$$\begin{bmatrix} f_d \\ f_q \\ f_0 \end{bmatrix} = T_{dq0}(\theta) \begin{bmatrix} f_a \\ f_b \\ f_c \end{bmatrix} \quad (2)$$

Variables f can be interpreted as a function of each phase's voltage, current, or motor flux. The magnitude $T_{dq0}(\theta)$ is described in the equation (9) [17] :

$$\left[T_{dq0}(\theta)\right] = \frac{2}{3}\begin{bmatrix} \cos\theta & \cos(\theta - \frac{2\pi}{3}) & \cos(\theta + \frac{2\pi}{3}) \\ \sin\theta & \sin(\theta - \frac{2\pi}{3}) & \sin(\theta + \frac{2\pi}{3}) \\ \frac{1}{2} & \frac{1}{2} & \frac{1}{2} \end{bmatrix} \quad (3)$$

And the inverse of $T_{dq0}(\theta)$ translated into equation (10) :

$$\left[T_{dq0}(\theta)\right]^{-1} = \begin{bmatrix} \cos\theta & \sin\theta & 1 \\ \cos(\theta - \frac{2\pi}{3}) & \sin(\theta - \frac{2\pi}{3}) & 1 \\ \cos(\theta + \frac{2\pi}{3}) & \sin(\theta + \frac{2\pi}{3}) & 1 \end{bmatrix} \quad (4)$$

TABLE I
PARAMETERS AND DATA SPECIFICATIONS OF THE INDUCTION MOTOR

No	Parameter	Value
1	Rated power (kW)	7.5
2	Rated Voltage (V)	400
3	Rated Frequency (Hz)	50
4	Rated Current (A)	14
5	Rated Speed (Rpm)	1440

B. ANFIS Training Stage and Identification Test

ANFIS (Adaptive Neuro Fuzzy Inference System) is an architecture that operates equivalently to Sugeno's fuzzy rule basis model [18]. The architecture of ANFIS resembles that of a neural network utilizing a radial basis function, subject to specific constraints [19]. ANFIS is a method that use a learning algorithm to optimize the rules based on a dataset [20]. ANFIS facilitates the adaptation of rules. To ensure that a radial basis function network emulates a fuzzy rule-based model, it must incorporate its architecture and processing to reflect the logical framework of fuzzy systems, wherein inputs are categorized and correlated to outputs according to established rules. This entails adjusting the network's settings to ensure its behavior corresponds with the interpretative and decision-making processes characteristic of fuzzy models [21]. For Sugeno order 1, the following constraints are necessary:

1. All outputs must have a uniform aggregate mechanism for the rules.
2. In a system with fuzzy rules (IF-THEN expressions), the number of activation functions should match the number of rules.
3. Each activation function must match the membership function associated with each distinct input when there are several inputs inside the rule base.
4. Activation functions and fuzzy rules must serve identical purposes for neurons and rules on the output side.

The ANFIS network comprises multiple layers, with each neuron in the initial layer adapting to the parameters of the activation function [22]. The αA1(x1), αB1(x2), αA2(x1), or αB2(x2) membership degrees are the outputs of each neuron, which are determined by the input membership function [23]. In this context, the commonly used types of membership functions include trimf, trapmf, gbellmf, gaussmf, gauss2mf, pimf, dsigmf, and product psigmf functions. Each of these functions serves a specific purpose in fuzzy systems by representing different shapes and behaviors for input-output relationships, allowing for flexible and accurate modeling of data patterns [24].

The triangular (trimf) membership function is characterized by a triangular form and is defined by three parameters: a, b, and c, denoting the starting point, the vertex, and the endpoint of the triangle, respectively. The membership function employed is of the triangular (trimf) kind, as delineated in formula (11) below [12] :

$$f(x,a,b,c) = \begin{Bmatrix} 0, & x \le a \\ \frac{x-a}{b-a}, & a \le x \le b \\ \frac{c-x}{c-b}, & b \le x \le c \\ 0, & c \le x \end{Bmatrix} \quad (11)$$

In graphical form it is depicted as Figure 3.

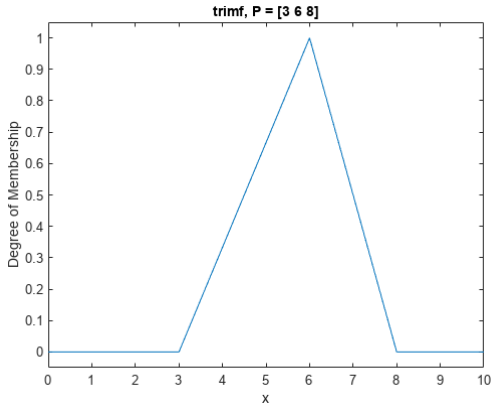

Figure 3 Trimf function graph

C. Model Training

It is at this stage of ANFIS processing that it can be used and is ready to run for training data that has been prepared previously. Until the parameter results are as follows:
Number of nodes: 55
Number of linear parameters: 80
Number of nonlinear parameters: 24
Total number of parameters: 104
Number of training data pairs: 400001
Number of checking data pairs: 0
Number of fuzzy rules: 16
Here's the anfis secture design:

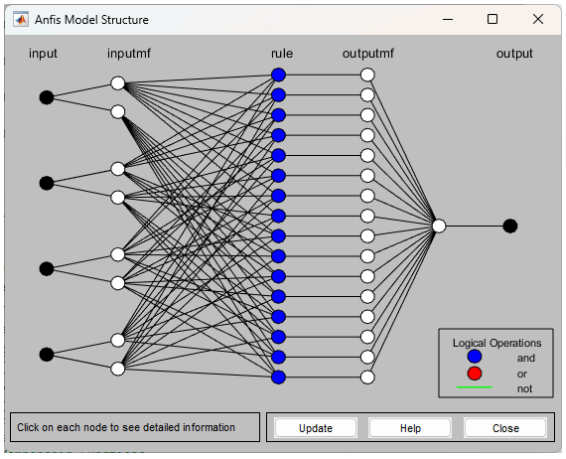

Figure 4 Neuro Fuzzy Structure

The design of the ANFIS, a model that combines artificial neural networks with fuzzy logic, is shown in Figure 3 [5]. This framework illustrates the progression of information from the input layer to the output over multiple phases. On the left, an input layer links input variables to multiple membership functions (inputmf) for the fuzzification process, transforming the precise input value into a fuzzy set. After that, these membership functions are applied to the inputs in the second layer. In the middle, blue nodes represent fuzzy rules formed from combinations of input membership functions, where each rule uses logical operations such as AND, OR, and NOT, which are represented by colour codes in the legend [25].

Next, the output membership function layer (outputmf) connects the fuzzy rules with the output membership function, performing a defuzzification process that converts the fuzzy set back into a strict value. Finally, the output layer calculates the final result which becomes the output of the ANFIS system after processing the input through fuzzy rules and membership functions. This ANFIS structure is important in learning and decision-making, It

employs the learning mechanism of artificial neural networks to optimize the rules and membership functions, enabling the system to address complicated and non-linear issues more efficiently.

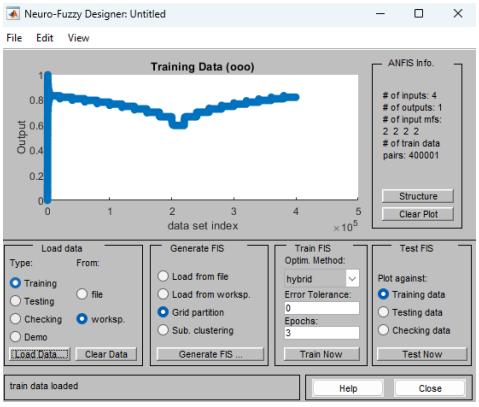

Figure 5 anfisedit data training

Figure 4 illustrates the Neuro-Fuzzy Designer interface utilized for constructing and training the ANFIS (Adaptive Neuro-Fuzzy Inference System). The graph displays the training data, with the X-axis representing the data index and the Y-axis denoting the output. This graph illustrates the output data's behavior in relation to changes in the data index, mirroring the pattern of the training data intended for the ANFIS model construction [26].

To the right, there is information regarding the ANFIS architecture, including the quantity of inputs, outputs, and membership functions utilized throughout the training process. The 'ANFIS Info' column indicates the presence of 4 inputs, 1 output, 2 membership functions per input, and a cumulative total of 400,001 training data pairs.

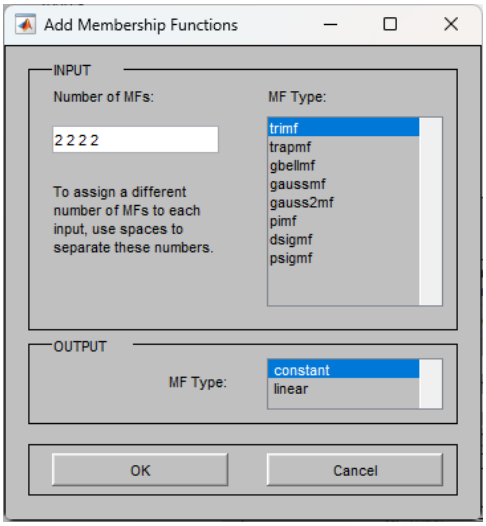

Figure 6 setting Member functions

Figure 5 shows the interface for adding membership functions in the ANFIS (Adaptive Neuro-Fuzzy Inference System) system. In this section, the user can set the number and type of membership functions for the input and output of the model.

In the input section, the user can specify the number of membership functions (MFs) to be applied to each input. In the 'Number of MFs' column, it can be seen that the number of membership functions for the four inputs has been specified, each having two membership functions (indicated by 2 2 2). The user can also set the type of membership function to be used, with options available on the right, such as trimf (Triangular Membership Function), trapmf (Trapezoidal Membership Function), and various other fuzzy membership functions, such as gaussmf (Gaussian) and pimf (Pi-shaped).

For output, the user can select the type of membership function for the model output. In this case, the two options available are constant and linear. This output membership function will be used to define how the result of the ANFIS model is mapped to a crisp value.

D. Evaluation

This evaluation model analyses the results of training that has been done with parameters. Root Mean Square Error (RMSE) is used to calculate the amount of error in predicting data. RMSE calculates the difference between the actual value and the expected value and divides the total sum obtained by the number of prediction times and draws the root. The Root Mean Square Error (RMSE) calculation can be seen in the following equation [27].

$$RMSE = \sqrt{\frac{\sum_{i=1}^{n}(y_i - \dot{y}_i)^2}{n}} \qquad (9)$$

III. RESULT AND DISCUSSION

A This section discusses the experimental results of the ANFIS model.

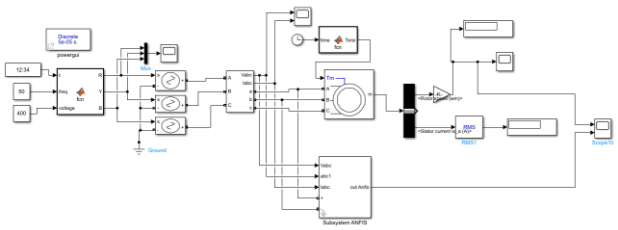

Figure 7 Simulation applied

Figure 6 simulates the anfis system made with 4 inputs, namely Vd, Vq, Id and Iq with motor speed output. As a replacement for the motor speed sensor.

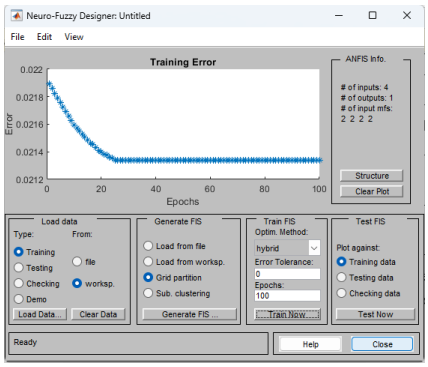

Figure 8 result training

Figure 7 training results with Based on having 4 inputs in the input there are 2 input member functions of type trapmf which will be set automatically after the training process. FIS that will be built then the Training process is carried out with epoch = 100. Simulation of Hybrid Algorithm with 'trapmf' function, with the number of MF [2 2 2 2], the output MF function is type 'constant'.

Table 2

Value RMSE

No	Mf Type	RMSE
1.	Trimf	0.0187
2.	Trapmf	0.0213
3.	Gbellmf	0.0193
4.	Gaussmf	0.0193

Table 2 above displays the RMSE values of several types of membership functions (Mf) used in the ANFIS system. The RMSE value measures the amount of error or variation between the actual value and the expected valueThe lower the RMSE value, the superior the model's performance in forecasting the anticipated output.

Based on the table, Trimf has the lowest RMSE value, which is 0.0187, indicating that this triangular membership function provides the most accurate prediction results. On the other hand, Trapmf (Trapezoidal Membership Function) has the highest RMSE value of 0.0213, indicating a greater prediction error than the other membership functions.

Moreover, the Gbellmf (Generalised Bell Membership Function) and Gaussmf (Gaussian Membership Function) exhibit identical RMSE values of 0.0193, indicating their equivalent efficacy in output prediction. Nonetheless, their prediction accuracy remains somewhat inferior to that of Trimf.

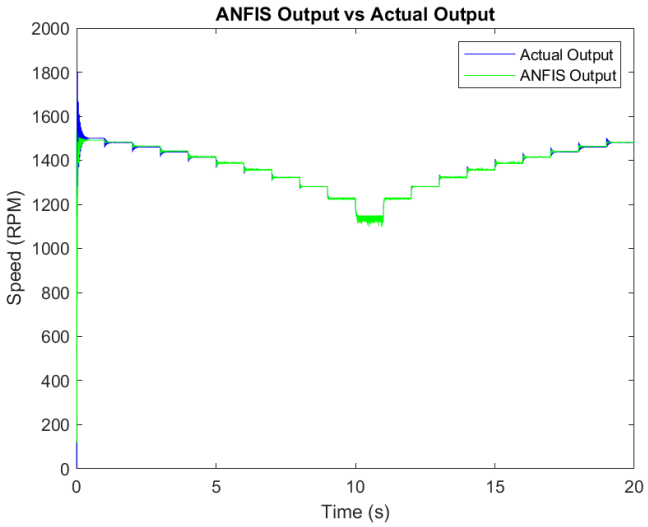

Figure 9 Speed actual and anfis Trimf

Figure 9 The graph above shows the comparison between ANFIS output and actual output in the form of rotational speed (RPM) against time (s). On the horizontal axis, time is expressed in seconds (s), while the vertical axis represents speed (Speed) in units of rotations per minute (RPM). This graph illustrates the performance of the ANFIS system in predicting speed compared to the actual output of the system.

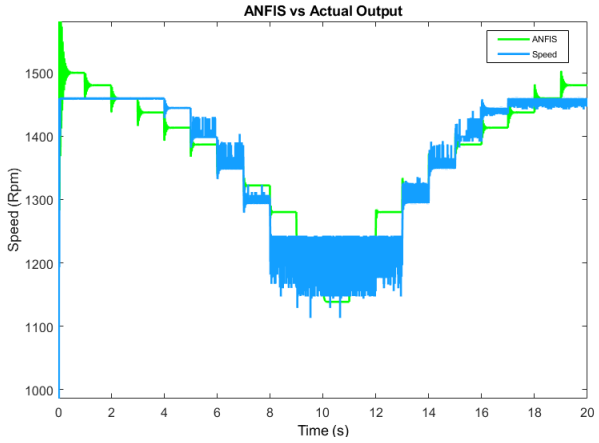

Figure 10 Speed actual and anfis Trapmf

Figure 10 presents a graph comparing the ANFIS output with the actual output in terms of rotational speed (RPM) over time (s). The horizontal axis represents time in seconds (s), while the vertical axis indicates speed in rotations per minute (RPM). The graph highlights the performance of the ANFIS system, which utilizes a trapezoidal membership function (Trapmf), in predicting rotational speed relative to the actual system output.

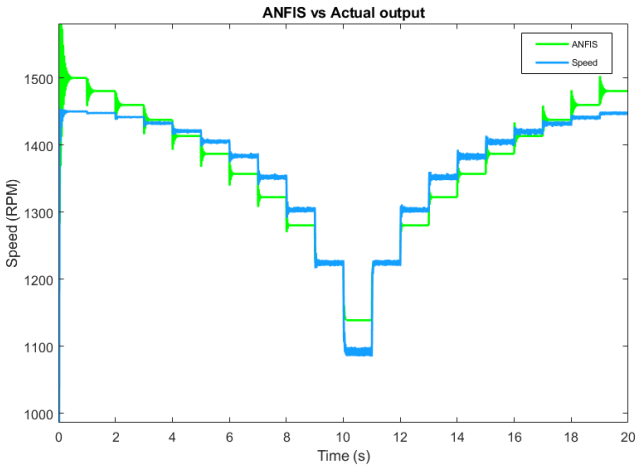

Figure 11 Speed actual and anfis Gbell

Figure 11 presents a graph comparing the ANFIS output with the actual output in terms of rotational speed (RPM) over time (s). The horizontal axis represents time in seconds (s), while the vertical axis indicates speed in rotations per minute (RPM). The graph highlights the performance of the ANFIS system, which utilizes a generalized bell-shaped membership function (Gbellmf), in predicting rotational speed relative to the actual system output.

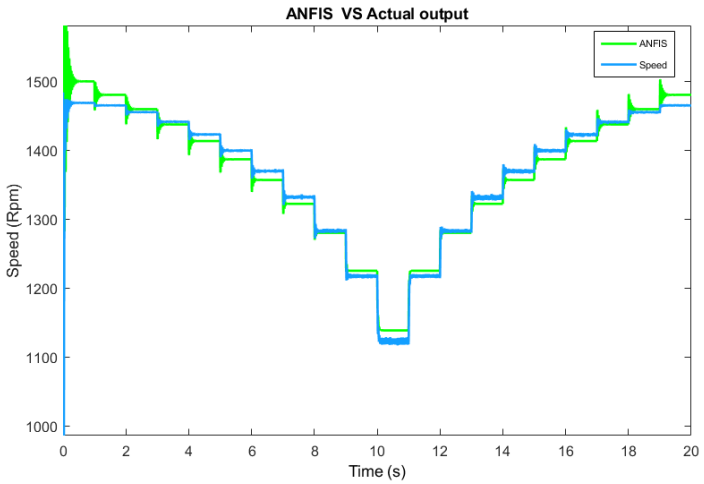

Figure 12 Speed actual and anfis Gaussmf

Figure 12 presents a graph comparing the ANFIS output with the actual output in terms of rotational speed (RPM) over time (s). The horizontal axis represents time in seconds (s), while the vertical axis indicates speed in rotations per minute (RPM). The graph highlights the performance of the ANFIS system, which utilizes a Gaussian membership function (Gaussmf), in predicting rotational speed relative to the actual system output.

The graph illustrates that the ANFIS output (depicted in green) and the actual output (depicted in blue) nearly coincide throughout the simulation duration, indicating the ANFIS model's capacity for precise speed prediction. At the beginning of the simulation, both the ANFIS output and the actual output show rapid speed changes. After that, the system experiences a decrease in speed at around 5 seconds to the lowest point before gradually increasing again.

Despite minor swings of 5-10 seconds, the disparity between the ANFIS output and the actual output is negligible, demonstrating that the ANFIS system effectively emulates the actual speed change pattern. This commendable result illustrates ANFIS's capacity to adjust the control system according to the received inputs while minimizing prediction error.

Overall, this graph indicates that the ANFIS model applied to the speed control system successfully predicts the output with a high degree of accuracy, although there are some small deviations in certain time periods.

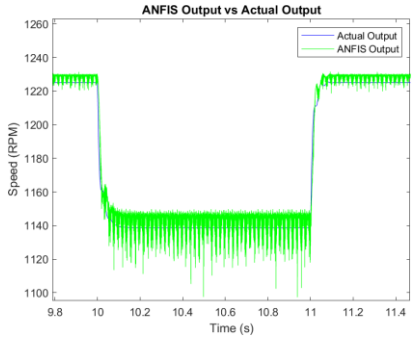

Figure 13 Graphical results of maximum load

The graph shows significant fluctuations in the ANFIS output. This could be caused by noise in the training data or test data. This noise can affect the ability of the ANFIS to correctly predict the speed of the induction motor. The fluctuations seen in the ANFIS output can also be caused by numerical instability in the training algorithm or during model evaluation. This often occurs if there are problems in handling very small or very large numbers.

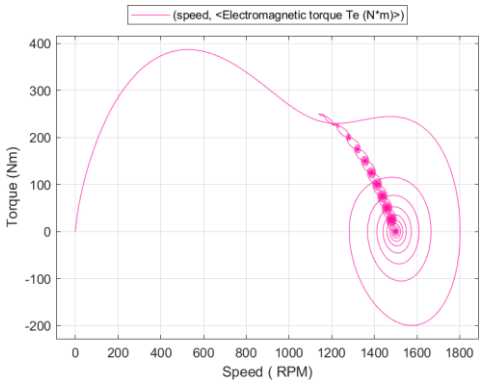

Figure 14 XY Graph Results

The above graph shows the relationship between electromagnetic torque (Nm) and speed (RPM) of a three-phase motor. This relationship is represented by the pink-coloured line, which illustrates how torque and speed change during motor operation. Spiral Pattern The spiral pattern seen in the graph shows the dynamic response of the motor to changes in speed and torque. This pattern indicates the presence of a damping effect that causes the motor to oscillate before reaching a steady state. The shrinking of the spiral indicates that the system is reaching stability and oscillations are decreasing.

Table 3 Member function plots fuzzy trimf

Fis variable	Before training	After training
Input 1	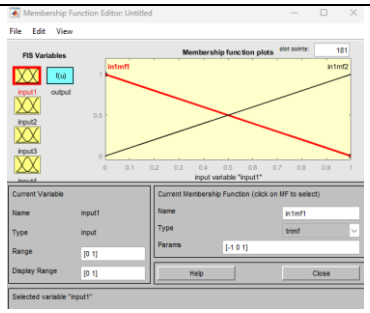	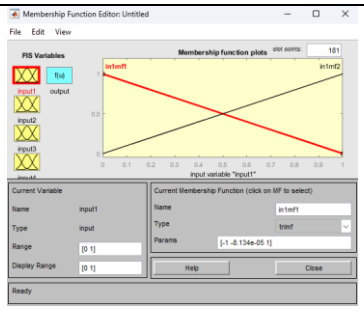

Input 2	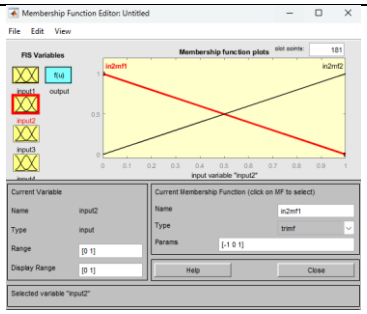	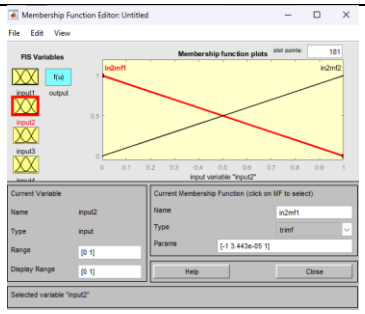
Input 3		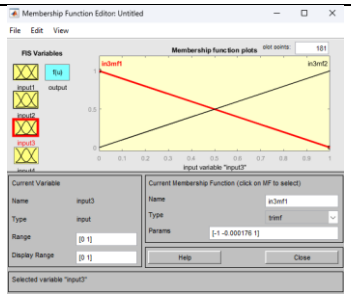
Input 4	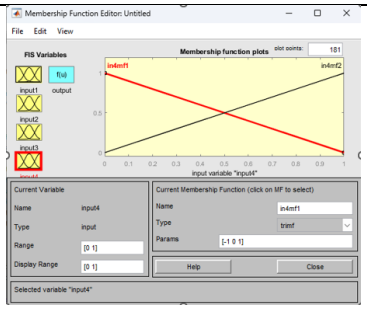	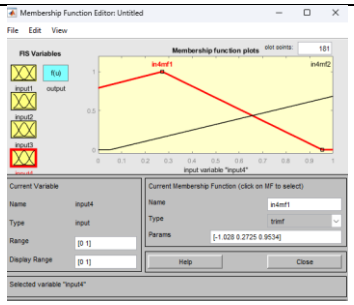

Table 4

Member function plots fuzzy trapmf

Fis variable	Before training	After training
Input 1	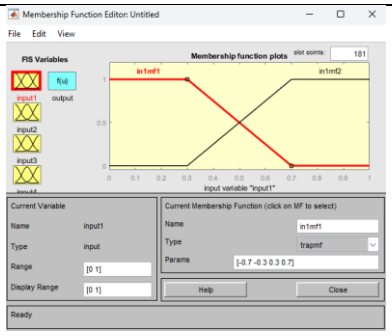	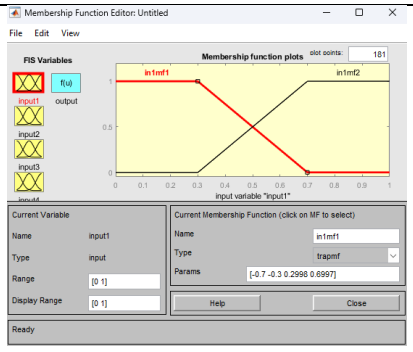
Input 2	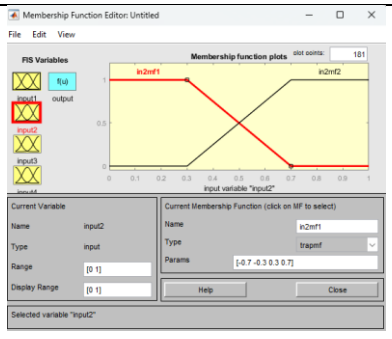	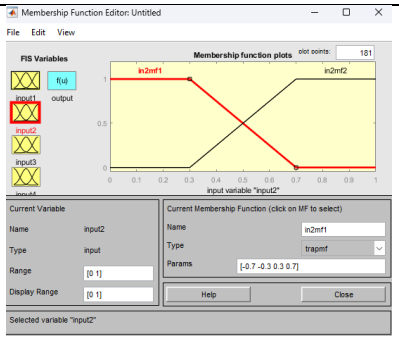

Input 3	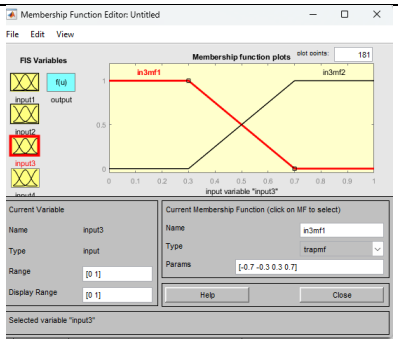	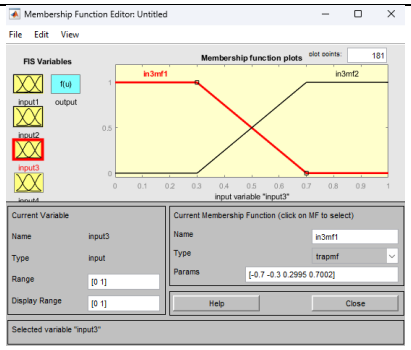
Input 4	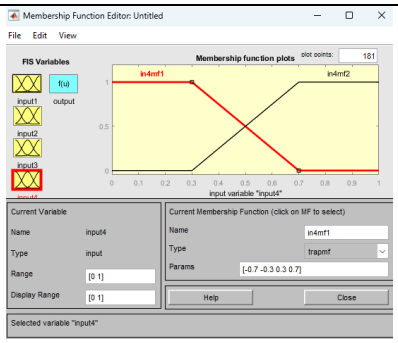	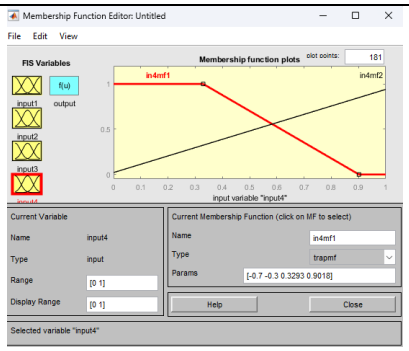

Table 5 Member function plots fuzzy gbellmf

Fis variable	Before training	After training
Input 1	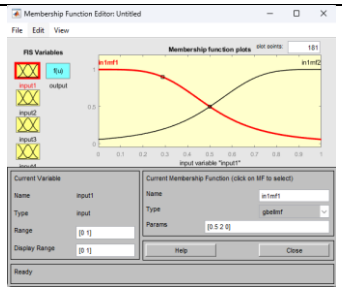	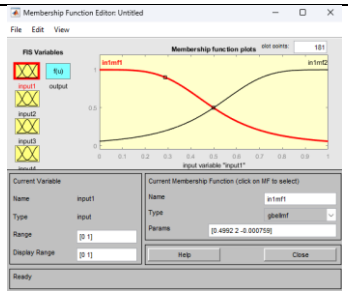
Input 2	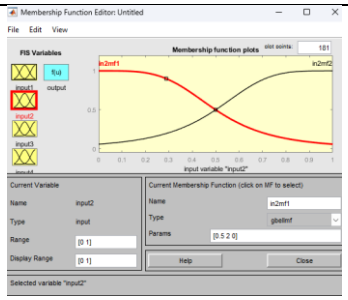	
Input 3		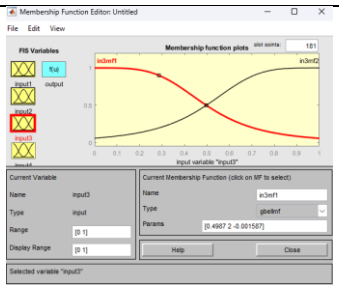

Input 4	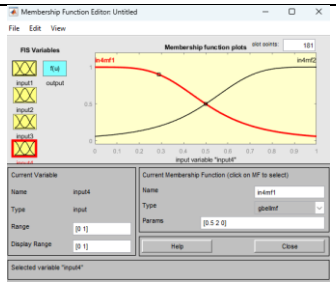	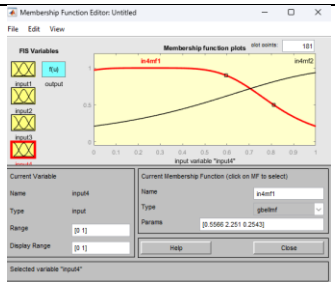

Table 6. Member function plots fuzzy gaussmf

Fis variable	Before training	After training
Input 1		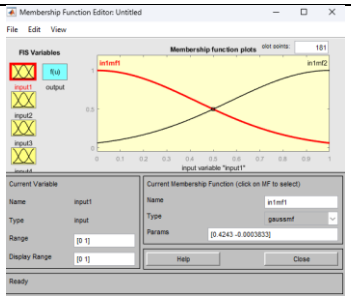
Input 2	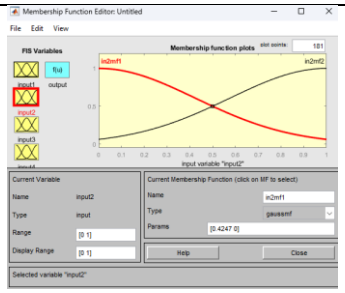	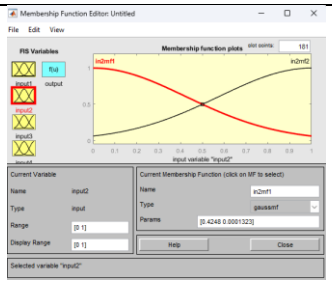
Input 3	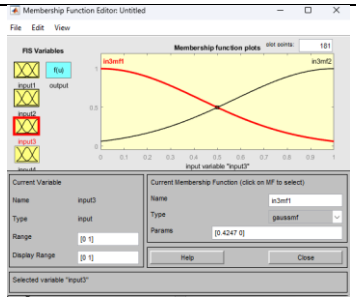	
Input 4	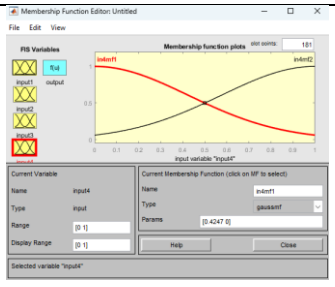	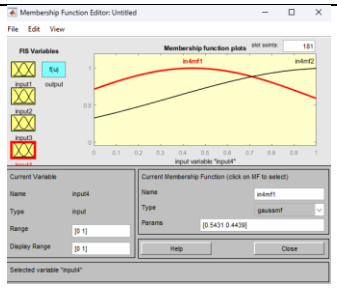

Based on Table 3,4, 5 and 6 the system utilizes four input variables, each consisting of two membership functions, which are initially set before training and automatically adjusted during the training process. The designed FIS undergoes a training phase with 100 epochs to optimize its performance. The Hybrid Algorithm simulation employs different types of membership functions, including triangular (Trimf), trapezoidal (Trapmf), generalized bell-shaped (Gbellmf), and Gaussian (Gaussmf), with the number of MFs set as [2 2 2 2], while the output MF function is defined

as ‘constant’. Before training, all membership functions are symmetrically distributed based on predefined parameters. However, after training, adaptive modifications occur in the membership functions, as reflected in the results shown in Table 4. These changes indicate the system’s ability to learn and dynamically adjust the MF parameters, demonstrating how different MF types respond to the training process and contribute to improving prediction accuracy.

Furthermore, a comparative analysis based on Tables 3, 4, 5, and 6 evaluates different types of membership functions, namely triangular (Trimf), trapezoidal (Trapmf), generalized bell-shaped (Gbellmf), and Gaussian (Gaussmf), both before and after training. Each of these MFs exhibits distinct adaptive behavior during the learning process. Table 3 presents results for the triangular function, Table 4 for the trapezoidal function, Table 5 for the generalized bell-shaped function, and Table 6 for the Gaussian function. The comparison highlights significant parameter shifts after training, demonstrating how each MF type adapts to the data. Trimf exhibits the highest predictive accuracy after training, while Trapmf shows the least accuracy. These findings emphasize the impact of MF selection on model efficiency and the importance of adaptive learning in sensorless motor speed estimation.

IV. CONCLUSIONS

This study investigates the implementation of the ANFIS for determining induction motor speed without the use of physical sensors. ANFIS amalgamates the capabilities of fuzzy logic with artificial neural networks to produce accurate motor speed predictions in the presence of uncertainty and fluctuations in motor parameters. This study demonstrates that the ANFIS method can supplant conventional sensor-based techniques, offering cost savings and enhanced resilience to environmental disruptions, aligning with the concepts of Industry 5.0.

The findings demonstrate that the trained ANFIS model can generate motor speed predictions with considerable accuracy, as reflected by the RMSE value. Among the many membership functions employed, the Trimf (Triangular Membership Function) exhibited superior performance, achieving the lowest RMSE value of 0.0187, whilst the Trapmf (Trapezoidal Membership Function) demonstrated the least efficacy with an RMSE of 0.0213.

The decrease in motor speed as the applied load increases is also effectively compensated by the ANFIS system, as seen in the simulation and comparison between ANFIS output and actual output. Although there is a slight deviation at certain time periods, the difference remains minimal, which demonstrates the ANFIS' ability to adapt and minimise prediction errors.

Overall, this research proves that ANFIS is an efficient and effective solution for induction motor speed estimation in the modern industrial era, especially in industrial applications that require intelligent automation and energy savings.

Aknowldegement

This research was funded by a scholarship from Politeknik Elektronika Negeri Surabaya (PENS). The authors would like to express their gratitude for the financial support provided, which contributed to the successful completion of this study.

REFERENCES

[1] A. A. Manjare and B. G. Patil, “A Review: Condition Based Techniques and Predictive Maintenance for Motor,” in 2021 International Conference on Artificial Intelligence and Smart Systems (ICAIS), IEEE, Mar. 2021, pp. 807–813. doi: 10.1109/ICAIS50930.2021.9395903.

[2] M. Barut, R. Demir, E. Zerdali, and R. Inan, “Real-Time Implementation of Bi Input-Extended Kalman Filter-Based Estimator for Speed-Sensorless Control of Induction Motors,” IEEE Transactions on Industrial Electronics, vol. 59, no. 11, pp. 4197–4206, Nov. 2012, doi: 10.1109/TIE.2011.2178209.

[3] B. Kiani, B. Mozafari, S. Soleymani, and H. Mohammadnezhad Shourkaei, “Predictive torque control of induction motor drive with reduction of torque and flux ripple,” Bulletin of the Polish Academy of Sciences: Technical Sciences, vol. 69, no. 4, Aug. 2021, doi: 10.24425/bpasts.2021.137727.

[4] R. Yildiz, M. Barut, and R. Demir, “Extended Kalman filter based estimations for improving speed‐sensored control performance of induction motors,” IET Electr Power Appl, vol. 14, no. 12, pp. 2471–2479, Dec. 2020, doi: 10.1049/iet-epa.2020.0319.

[5] P. T. Giang, V. Q. Vinh, T. T. Van, and V. T. Ha, “Experiment on Sensorless Control of an Induction Motor using Backpropagation Neural Network,” International Journal of Engineering Trends and Technology, vol. 70, no. 10, pp. 87–97, Oct. 2022, doi: 10.14445/22315381/IJETT-V70I10P211.

[6] S. El Daoudi, L. Lazrak, N. El Ouanjli, and M. Ait Lafkih, “Sensorless fuzzy direct torque control of induction motor with sliding mode speed controller,” Computers & Electrical Engineering, vol. 96, p. 107490, Dec. 2021, doi: 10.1016/j.compeleceng.2021.107490.
[7] N. Wilcken and M. Grotjahn, “Rotor Position Estimation for Permanent Magnet Synchronous Machines using Electromotive Force and Anisotropy Using Extended-Kalman-Filter,” Forschung im Ingenieurwesen/Engineering Research, vol. 87, no. 2, pp. 767–776, Jun. 2023, doi: 10.1007/s10010-023-00660-z.
[8] X. Wang, Y. Zhang, and H. Yang, “An improved deadbeat predictive current control for induction motor drives,” IET Power Electronics, vol. 16, no. 1, pp. 1–10, Jan. 2023, doi: 10.1049/pel2.12358.
[9] H. Abu‐Rub, A. Iqbal, and J. Guzinski, High Performance Control of AC Drives with MATLAB®/Simulink. Wiley, 2021. doi: 10.1002/9781119591313.
[10] A. Varatharajan, G. Pellegrino, and E. Armando, “Self-Commissioning of Synchronous Reluctance Motor Drives: Magnetic Model Identification with Online Adaptation,” in 2020 IEEE Energy Conversion Congress and Exposition (ECCE), IEEE, Oct. 2020, pp. 5353–5360. doi: 10.1109/ECCE44975.2020.9236307.
[11] Y. Ding, “Comparative study on control effect of permanent magnet synchronous motor based on Fuzzy PID control and BP neural network PID control,” J Phys Conf Ser, vol. 1802, no. 3, p. 032080, Mar. 2021, doi: 10.1088/1742-6596/1802/3/032080.
[12] B. Nikmaram, S. A. Davari, P. Naderi, C. Garcia, and J. Rodriguez, “Sensorless Simplified Finite Control Set Model Predictive Control of SynRM Using Finite Position Set Algorithm,” IEEE Access, vol. 9, pp. 47184–47193, 2021, doi: 10.1109/ACCESS.2021.3068085.
[13] M. Korzonek, G. Tarchala, and T. Orlowska-Kowalska, “A review on MRAS-type speed estimators for reliable and efficient induction motor drives,” ISA Trans, vol. 93, pp. 1–13, Oct. 2019, doi: 10.1016/j.isatra.2019.03.022.
[14] M. A. Fnaiech, J. Guzinski, M. Trabelsi, A. Kouzou, M. Benbouzid, and K. Luksza, “MRAS-Based Switching Linear Feedback Strategy for Sensorless Speed Control of Induction Motor Drives,” Energies (Basel), vol. 14, no. 11, p. 3083, May 2021, doi: 10.3390/en14113083.
[15] S. Ravikumar and D. Kavitha, “IOT based autonomous car driver scheme based on ANFIS and black widow optimization,” J Ambient Intell Humaniz Comput, 2021, doi: 10.1007/s12652-020-02725-1.
[16] C. J. O’Rourke, M. M. Qasim, M. R. Overlin, and J. L. Kirtley, “A Geometric Interpretation of Reference Frames and Transformations: Dq0, Clarke, and Park,” IEEE Transactions on Energy Conversion, vol. 34, no. 4, pp. 168–17, Dec. 2019, doi: 10.1109/TEC.2019.2941175.
[17]S. Shah, A. Rashid, and M. Bhatti, “Direct Quadrate (D-Q) Modeling of 3-Phase Induction Motor Using MatLab / Simulink,” 2012.
[18] Widjonarko, A. Setiawan, B. Rudiyanto, S. B. Utomo, and M. M. Setiyo, “Characteristic of Fuzzy, ANN, and ANFIS for Brushless DC Motor Controller: An Evaluation by Dynamic Test,” International Journal of Integrated Engineering, vol. 13, no. 6, pp. 274–284, 2021, doi: 10.30880/ijie.2021.13.06.024.
[19] A. A. Menaem, M. Elgamal, A. H. Abdel-Aty, E. E. Mahmoud, Z. Chen, and M. A. Hassan, “A Proposed ANN-Based Acceleration Control Scheme for Soft Starting Induction Motor,” IEEE Access, vol. 9, pp. 4253–4265, 2021, doi: 10.1109/ACCESS.2020.3046848.
[20] A. Isqeel Abdullateef, M. Faiz Sanusi, and S. Fagbolagun, “Induction Motor Stator Fault Classification Using PCA-ANFIS Technique,” vol. 19, no. 1, pp. 33–40, 2020, [Online]. Available: www.elektrika.utm.my
[21] N. H. Mugheri and M. U. Keerio, “An Optimal Fuzzy Logic-based PI Controller for the Speed Control of an Induction Motor using the V/F Method,” 2021. [Online]. Available: www.etasr.com
[22] E. Purwanto, I. Ferdiansyah, S. Dwitya Nugraha, and O. A. Qudsi, “The Effect of ANFIS Controller on The Performance of Induction Motor Drives in Low-Speed Operation Based on IFOC,” vol. 11, no. 2, 2021.
[23] M. Babanezhad, I. Behroyan, A. Marjani, and S. Shirazian, “Artificial intelligence simulation of suspended sediment load with different membership functions of ANFIS,” Neural Comput Appl, vol. 33, no. 12, pp. 6819–6833, Jun. 2021, doi: 10.1007/s00521-020-05458-6.
[24] The MathWorks Inc., MATLAB version: 9.13.0 (R2022b). The MathWorks Inc., 2022. Accessed: Oct. 16, 2024. [Online]. Available: https://www.mathworks.com}
[25] A. Bhowate, M. Aware, and S. Sharma, “Predictive Torque Control with Online Weighting Factor Computation Technique to Improve Performance of Induction Motor Drive in Low Speed Region,” IEEE Access, vol. 7, pp. 42309–42321, 2019, doi: 10.1109/ACCESS.2019.2908289.
[26] T. Elgallai, “Fault Detection and Condition Monitoring in Induction Motors Utilizing Machine Learning Algorithms,” Brilliance: Research of Artificial Intelligence, vol. 4, no. 1, pp. 38–46, Mar. 2024, doi: 10.47709/brilliance.v4i1.3539.
[27] K. Vidhya and R. Shanmugalakshmi, “Modified adaptive neuro-fuzzy inference system (M-ANFIS) based multi-disease analysis of healthcare Big Data,” Journal of Supercomputing, vol. 76, no. 11, pp. 8657–8678, Nov. 2020, doi: 10.1007/s11227-019-03132-w.